SURFACE PROCESSES ASSOCIATED WITH LUNAR SWIRLS. P. H. Schultz[1] and M. Bruck Syal[2], [1]Brown University, Providence, RI 02912 (peter_schultz@brown.edu), [2]Lawrence Livermore National Laboratory, Livermore, CA 94551

Introduction: The lunar swirls remain a mystery. Whether due to the consequences of an ancient pre-existing field [1,2] or to the effects of cometary collisions [3,4], these looped bright and dark patterns are more than a curiosity. As a result of a remanent magnetic field, such patterns provide clues for the lunar dynamo. As a consequence of cometary collisions, they provide a unique signature of broad-scale interactions and a record of rare (yet probable) collisions that must have occurred within the last 10's of millions of years. This contribution focuses on surface processes inferred by their photometry and expressions on the surface that provides insight into their mode of formation.

Background: Early observations recognized the unique photometric properties and broad-scale distribution of lunar swirls, independent of any associated magnetic fields [3,5]: draping of pre-existing crater walls and rims; absence of visible alteration of the surface down to a scale of 10m; uniquely strong forward reflective properties (relative to unaffected regions); absence of any expression in the thermal inertia or radar data; lanes that are darker than unaffected regions (whether in the mare or the highlands); superposition on large Copernican crater ejecta deposits (e.g., King Crater); and a distribution independent of impact basins or antipodal regions [1,6]. The study by Blewett [6] provided an exhaustive inventory of the swirls and their characteristics, but here we re-examine the process of swirl formation in the context of observable surface process.

Photometry: Aside from their distinctive pattern, lunar swirls exhibit a distinctive photometric function. As well known to most amateur astronomers, the best-known swirl system on the lunar nearside (Reiner γ) seems to float above the surface as the Moon wanes, i.e., at very large phase angles (>130°), yet at near-full moon (low phase angles) swirls are just another higher albedo feature. This was recognized both telescopically and from early Lunar Orbiter images [5]. Direct telescopic observations of Reiner γ and early, well-calibrated photometric maps of the Moon over a lunation [7] formed the basis for the assertion that the lunar swirls must represent a physical alteration of the surface, not just a deposit [3]. Later studies documented this property over a more limited range of phase angles [e.g., 8, 9].

Figure 1 shows the brightness of the Reiner γ swirl subtracted from the brightness of an adjacent unaffected mare surface at different phase angles derived from [7]. Each reference value for the unaffected surface from the isophotic atlas was taken at the same local phase angle. For comparison, the same differences are shown for crater rays from Tycho and Copernicus (relative to adjacent maria). Reiner γ exhibits unique brightening as the phase angle changes from -80° to -10°; moreover, this brightness persists out to very large phase angles (+80°). At 60°, Reiner γ is more than 8 times brighter than are rays from Tycho and Copernicus, relative to unaffected surfaces.

Surface Processes: The LROC cameras now provide much more detailed views of different swirls and related processes, especially for Reiner γ and swirls near Mare Marginis (near Goddard-A, G-A). First, small craters within the dark lanes expose brighter materials beneath the surface (Reiner γ), whereas small craters within the brighter swirls do not excavate darker materials below. This observation suggests that the dark lanes represent a surface veneer, whereas the bright swirls represent physical alteration of the surface. Second, dark lanes "blacken" all sloped surfaces, e.g., crater walls (whether on the mare or highlands), thereby also implicating a surface veneer. Third, dark lanes and bright swirls extend down sloped surfaces. This observation requires that the process forming the swirls occur at the micron to mm scale, without causing significant mobilization (slope failure). Fourth, dark lanes in swirls superpose near-rim ejecta facies of G-A, whereas distal crater rays from cross the dark lanes (Fig. 2). Hence, the swirls formed both before and after the Goddard-A impact, i.e., during the collision.

Goddard-A is not the only crater associated with a swirl pattern. A 15km-diameter crater (Mandel'shtam F, M-F) on the farside highlands exhibits a zone of avoidance (ZoA) to the NW (Fig. 3) where the uprange rim of M-F extends down a local slope. A set of compositionally distinct rays extend to the NW where a localized patch of swirls occur 90 km away, with a diffuse bright zone 60 km still farther. These swirls correlate with the tops of facing topographic highs, whereas the bright zone has no particular association. In both regions, the highest resolution LROC images reveal no clear surface expression, other than possible roughening at the limit of resolution. We interpret this swirl and bright zone as expressions of interactions between the surface relief and an impact-generated vapor plume escaping from the breached rim of M-F. Similar topographic effects occur in certain other swirls. This association illustrates the role of surface interactions with impact vapor to create swirl patterns.

Other Properties: In addition to their unique photometric function, swirls exhibit distinctive signatures in spectral maturity [10], UV/VIS image

ratios [11], and polarization [12]. Early studies argued that swirls represent immature surfaces due to the inferred lower FeO signature in the high-reflectance component of the swirls [6]. More recent studies [10], however, indicate characteristics inconsistent with typical optical maturity trends across on- and off-swirl regions; instead, the high-reflectance regions must represent physical alteration of the regolith structure, consistent with prior conclusions [3]. The bright swirls also exhibit low UV/VIS (321nm/415nm) ratios similar to melt deposits on the inner rim of Giordano Bruno [12], indicative of glassy materials [12,13]. Finally, polarization measurements further underscore the conclusion that the swirls correspond to surfaces with different physical properties [12], e.g., a strong backscatter region (eastern Reiner γ) correlating with slopes on wrinkle ridges.

Mercurian Swirls: Bright patches on Mercury from Mariner 10 images were initially proposed as analogs for lunar swirls [3] where cometary nuclei dominate the impactor flux. The MESSENGER mission revealed, however, that lunar-like swirls did not exist [14]. This result should not be considered evidence against the cometary origin for swirls for two reasons. First, the proximity of Mercury to the Sun results in much higher space weathering effects that can rapidly mask albedo contrast within the upper few mm on Mercury. Second, higher impact speeds at Mercury generate more vaporization with higher expansion speeds. Their rapid expansion may prevent the formation swirls. However, scouring by the interactions between the coma and impact vapor near the impact could account for the strong forward-scattering haloes around small fresh craters on Mercury that contrast with lunar craters.

Implications: Based on the observations, the high-reflectance swirl pattern must be the result of a localized smoothing of the surface at micron to mm scales, inconsistent with the shielding of the solar wind or deposition of fines. While a local magnetic field might shield the regolith from proton bombardment, it could not shield surface from the micrometeorite impact flux. Focused planetary missions addressing the depth of magnetic sources and nature of the surface materials could resolve the true mode of origin.

References: [1] Hood, L. L., and C. Williams (1989), *Proc. Lunar Planet. Sci. Conf. 19th*, 99–113; [2] Garrick-Bethell, I. et al. (2011) Icarus 212, 480-492; [3] Schultz and Srnka (1980) Nature 284, 22-26; [4] Bruck-Syal et al. (2013), LPSC 44, #2569; [5] Schultz, P. H. (1976), *Moon Morphology*, U. Texas Press, 626 pp;[6] Blewett, D.T. et al. (2011*), J. Geophys. Res.-Planet. 116*, 2002; [7] Saari, J. M. and Shorthill, R. W. (1967), *NASA Contractor Report* NASA CR-855; [8] Shkuratov, Y. et al. (2010), Icarus *208*, 20–30; [9] Kaydash, V. et al. (2009), Icarus 202, 393–413; [10] Pieters, C. P. *et al*. (2014), *LPSC 45*, #1408; [11] Denevi, B. W. (2011), EPSC-DPS2011-1238; [12] Wöhler, C. (2008), LPSC 39, #1123; [13] Cloutis, E. A. et al. (2008), *Icarus* 197, 321-347; [14] Blewett, D. T. et al. (2010), *Icarus* 209, 239-246.

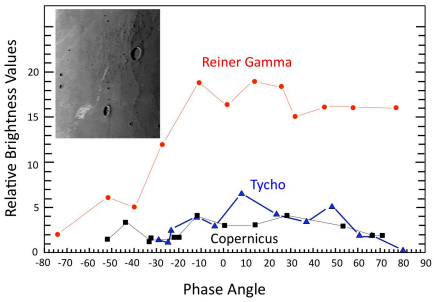

Fig. 1: Effect of phase angle on relative brightness of Reiner γ and crater rays relative to unaffected mare surfaces The inset shows a telescopic view Reiner γ at a large phase angle.

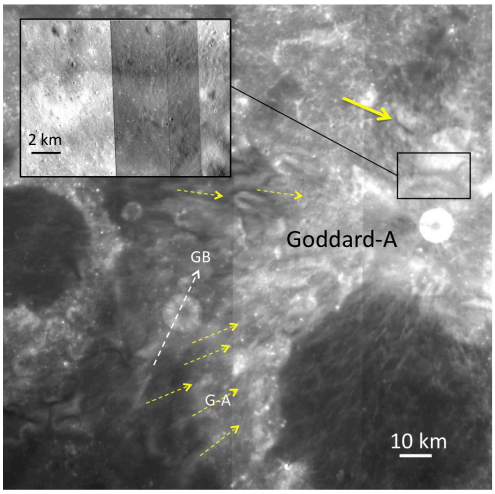

Fig. 2: Age relation between swirls and rays from Goddard A (G-A) and Giordano Bruno (G-B). Swirls both occur on top (inset) and below (yellow arrows) ejecta from G-A; hence, they were part of G-A's formation. Rays from G-B cross the bright and dark swirls, indicating a younger age.

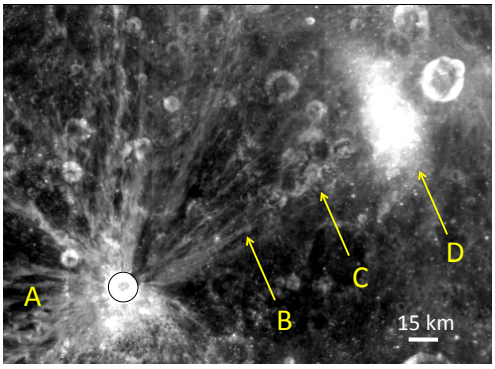

Fig. 3: The 17km-diameter crater Mandel'shtam F (A) on the lunar farside (5.2°N, 166.2°E) with rays (B), swirls (B), and a more distal bright zone (D) attributed to high-speed vapor interactions with the surface.